Journal of Environmental Science and Health, Part B
Publication details, including instructions for authors and subscription information:
http://www.informaworld.com/smpp/title~content=t713597269

Enhanced visual detection of pesticides using gold nanoparticles

Kinattukara Parambil Lisha[a]; Anshup[a]; Thalappil Pradeep[a]
[a] Department of Chemistry and Sophisticated Analytical Instrument Facility, Indian Institute of Technology Madras, Chennai, India

To cite this Article Lisha, Kinattukara Parambil , Anshup and Pradeep, Thalappil(2009) 'Enhanced visual detection of pesticides using gold nanoparticles', Journal of Environmental Science and Health, Part B, 44: 7, 697 — 705
To link to this Article: DOI: 10.1080/03601230903163814
URL: http://dx.doi.org/10.1080/03601230903163814

Journal of Environmental Science and Health Part B (2009) **44**, 697–705

ISSN: 0360-1234 (Print); 1532-4109 (Online)
DOI: 10.1080/03601230903163814

Taylor & Francis
Taylor & Francis Group

Enhanced visual detection of pesticides using gold nanoparticles

KINATTUKARA PARAMBIL LISHA, ANSHUP and THALAPPIL PRADEEP

Department of Chemistry and Sophisticated Analytical Instrument Facility, Indian Institute of Technology Madras, Chennai, India

The presence of parts per billion (ppb) levels of chlorpyrifos (*O*, *O*-Diethyl-*O*-(3,5,6-trichloro-2-pyridyl) phosphorothioate) and malathion (*S*-1,2-bis(ethoxycarbonyl) ethyl *O*, *O*-dimethyl phosphorodithioate), two common pesticides found in the surface waters of developing countries, have been visually detected using gold nanoparticles. Visual detection of the presence of pesticide is possible when the color change occurring by the adsorption of pesticides on gold nanoparticles is enhanced by sodium sulfate. The method presented here is simple and there is no need of sample preparation or preconcentration. The response occurs within seconds and the color change is very clear. The detection is possible if chlorpyrifos and malathion are present up to a concentration of 20 and 100 ppb, respectively. The method shows great potential for on-site pesticide monitoring. The method is also applicable as a qualitative technique for the performance evaluation of various household water filters, which claim pesticide removal.

Keywords: Water; gold nanoparticles; chlorpyrifos; malathion; sodium sulfate.

Introduction

Chlorpyrifos is a broad-spectrum organophosphorus insecticide, widely used for crop protection and mosquito control. It can act as an inhibitor for cholinesterase enzyme, an enzyme that catalyzes the hydrolysis of neurotransmitter acetyl choline into choline and acetic acid. Once cholinesterase enzyme is inactivated, acetyl choline will accumulate in nervous system which results in over stimulation of acetyl choline receptors. This will result in disorders in the central nervous system, cardiovascular system and respiratory system.[1] Malathion is a degradable pesticide which breaks down in the environment by hydrolysis, biodegradation and photolysis.[2] It is suspected to cause kidney problems, human birth defects and child leukemia.[3] Water pollution due to pesticides is a critical problem in developing countries. Several methods exist to monitor the presence of pesticides in water samples. Established techniques, such as liquid and gas chromatography and mass spectrometry provide limits of detection at the ppb level.[4–7] These techniques are highly sensitive but time consuming and expensive. Demand for trained technicians for the analysis and the difficulty in on-site or in-field applications are some of the limits of these techniques, although portable devices are available. Biosensors are also explored for the detection of organophosphate pesticides in water.[8–10]

Gold nanoparticles are highly attractive materials for optical applications due to the localized surface plasmon resonance (LSPR). It is the collective oscillation of surface electrons induced by visible light which results in an extinction band in the visible region of the optical spectrum. The extinction band can be tuned by the particle size, shape and structure as well as the distance between the particles, refractive index of the surrounding medium and presence of adsorbed molecules on the particle surface. The intense red color of aqueous gold solution is an expression of LSPR.[11,12] Gold nanoparticles have been effectively utilized for the detection of many pollutants present in the environment. Mercury has been detected in water samples by various research group using different types of gold nanoparticles.[13–16] Similarly, the presence of copper ions in water samples has been detected by azide and terminal alkyne-functionalized gold nanoparticles.[17] Our group has already shown the possibility to detect endosulfan at parts per million (ppm) levels using gold nanoparticles.[18] Gold nanoparticles are covalently coupled with acetylcholinesterase (AChE) to create a biosensor and have been used for the detection of paraoxon.[19] AChE electrode was

Address correspondence to Thalappil Pradeep, DST Unit on Nanoscience (DST UNS), Department of Chemistry and Sophisticated Analytical Instrument Facility, Indian Institute of Technology Madras, Chennai 600 036, India; E-mail: pradeep@iitm.ac.in or pradeep@IITM.AC.IN
Received September 10, 2008.

stabilized by an electrodeposited gold nanoparticle layer and has been used for the detection of carbofuran.[20] A stable AChE biosensor, formed by the assembly of gold nanoparticles on a sol-gel derived silicate network for immobilization of AChE has been investigated for the detection of monocrotophos, methyl parathion and carbaryl.[21] AChE was immobilized on gold nanoparticle-chitosan interface and was tested for the detection of malathion.[22] Gold nanoparticle-based surface enhanced fluorescence has been studied for the detection of organophosphorus agents by Dasary et al.[23]

Here we make use of the color change of gold nanoparticles from red to blue by salt induced aggregation for the monitoring of the presence of two common pesticides, chlorpyrifos and malathion, in ppb levels. The developed method is very simple and doesn't need any expensive chemicals. The response is very fast and observable to the naked eye. It doesn't demand laborious sample preparation and can be done by inexperienced hands. This colorimetric method can be effectively utilized for on-site monitoring of pesticides. The key to this detection strategy is to make the nanoparticle system sensitive by the addition of a suitable salt.

Materials and methods

Chemicals used

Technical grade chlorpyrifos (*O*, *O*-Diethyl-*O*-(3,5,6-trichloro-2-pyridyl) phosphorothioate) and malathion (*S*-1,2-bis(ethoxycarbonyl) ethyl *O*, *O*-dimethyl phosphorodithioate) were purchased from Tropical Agro Systems (India Limited). Stock solutions (100 ppm) of each pesticide were prepared in 2-propanol. These solutions were diluted in water and used for further experiments. Tetrachloroauric acid trihydrate ($HAuCl_4.3H_2O$) was purchased from CDH India. Trisodium citrate was purchased from SRL India and used as received. Sodium sulfate (Na_2SO_4), sodium chloride (NaCl), potassium sulfate (K_2SO_4), ammonium sulfate ($(NH_4)_2SO_4$) and silver nitrate ($AgNO_3$) were purchased from E. Merck India Limited. Activated alumina was purchased from a local source. Triply distilled water was used throughout the experiment.

Instrumentation

Ultraviolet-visible (UV-vis) absorption spectra were measured on a Perkin-Elmer Lambda 25 spectrometer. High Resolution Transmission Electron Microscopy (HRTEM) was carried out using a 300 kV JEOL-3011 instrument with a ultra high resolution (UHR) polepiece. The samples for HRTEM were prepared by dropping the dispersion on amorphous carbon films supported on a copper grid and dried in ambience. Scanning Electron Microscopic (SEM) image was taken using a FEI QUANTA-200 SEM instrument. For the SEM measurement, the sample was drop-casted on an indium tin oxide (ITO) conducting glass and dried.

Synthesis of gold nanoparticles

Gold nanoparticles (Au@citrate) with an average diameter of 10–20 nm were synthesized by the reduction of $HAuCl_4.3H_2O$ with trisodium citrate.[24] In this method, 10 mL of 5 mM $HAuCl_4.3H_2O$ was diluted with 180 mL of distilled water and heated until it begins to boil. An amount measuring 10 mL of 0.5% trisodium citrate solution was added and continued heating until the solution turned wine red. It was cooled under ambient conditions.

Synthesis of silver nanoparticle supported on alumina

Silver nanoparticles with an average diameter of 40–60 nm were synthesized by the citrate reduction method.[25] In this method 500 mL of 1 mM $AgNO_3$ solution was allowed to boil. An amount measuring 20 mL of 1% trisodium citrate solution was added into this and continued heating until the solution turned pale yellow. It was cooled in a water bath. Supported silver nanoparticles were prepared by the following procedure. An amount measuring 10 g of neutral activated alumina was soaked in 25 mL of silver nanoparticle suspension well for 10 minutes and allowed to stand for half an hour. The supernatant became colorless. It was replaced with another fresh 25 mL suspension. This procedure was repeated until there was no color change for the supernatant. After decanting the supernatant, silver nanoparticle-coated alumina were washed thoroughly with distilled water and dried under ambient condition. The silver loading on alumina was 2200 ppm.

UV-vis analysis and colorimetric detection

Two mL of 5000 ppm Na_2SO_4 solution was mixed with 1 mL of Au@citrate. To this 1 mL of chlorpyrifos or malathion solution was added and the color change was noted. The chlorpyrifos concentrations used in the experiment were 12, 25, 125 and 250 ppb, respectively. The malathion concentrations used in the experiment were 25, 125, 250 and 500 ppb, respectively. A control experiment was done with water instead of the pesticide solution.

The absorption spectra of the samples before and after the pesticide addition were recorded at a wavelength of 400–900 nm.

For finding the effect of Na_2SO_4 on the color change, pesticide solution was added to Au@citrate and the absorption spectrum was measured. Effect of other salts such as NaCl, K_2SO_4 and $(NH_4)_2SO_4$ instead of Na_2SO_4 on the enhanced detection of pesticide was also studied.

Analysis of real water

The performance of the system in a complex environment was studied using ground water samples collected from Chennai, India. This sample was spiked with the two pesticides chosen for the present study. Colorimetric detection was done with 20 and 25 ppb chlorpyrifos and 100 and 125 ppb malathion.

Detection of treated samples

In order to study the effectiveness of this colorimetric detection for practical applications, 1 ppm chlorpyrifos solution was passed through a syringe filter containing 1 g of silver nanoparticle-coated alumina. The input was tested for pesticide. The output was collected at an interval of 10 mL and tested for pesticide. The real water sample spiked with a mixture of 1 ppm each chlorpyrifos and malathion was passed through silver nanoparticle-coated alumina column and colorimetric detection of the filtrate was carried out.

HRTEM and SEM analyses

For understanding the structural and morphological changes, HRTEM analysis of Au@citrate and Au@citrate/Na_2SO_4 mixture with and without chlorpyrifos were done. SEM analysis of the Au@citrate/Na_2SO_4 mixture with chlorpyrifos was done for understanding the morphology.

Results and discussion

UV-vis analysis and colorimetric detection

Detection of chlorpyrifos and malathion in different water samples followed colorimetric methods and the results are depicted in Figures 1 to 5.

UV-vis spectra of the Au@citrate before and after the addition of chlorpyrifos showed significant variation. Figure 1A shows the UV-vis spectra of Au@citrate and Au@citrate/Na_2SO_4 mixture before and after chlorpyrifos addition. Trace 'a' is the UV-vis spectrum of Au@citrate and it exhibits a characteristic absorption at 520 nm due to surface plasmon resonance. Trace 'b' is the UV-vis spectrum of Au@citrate/Na_2SO_4 mixture. Trace 'c' is the UV-vis spectrum of 12 ppb chlorpyrifos in Au@citrate/Na_2SO_4 mixture. Traces 'd-f' are the UV-vis spectra of 25, 125 and 250 ppb chlorpyrifos in Au@citrate/Na_2SO_4 mixture, respectively. Traces 'b' and 'c' are almost the same and they showed plasmon absorption at 526 nm, a slight difference from the Au@citrate as prepared. This may be due to the aggregation of nanoparticles by the adsorption of cationic species on the surface.[26] For 12 ppb chlorpyrifos, low concentration may be responsible for the lack of significant change from Au@citrate/Na_2SO_4 absorption spectrum. But from 25 ppb onwards the intensity of the plasmon absorption at 526 nm decreased and another broad plasmon emerged at longer wavelength. The plasmon at longer wavelength showed red shift and an increase in intensity with increase in concentration. The emergence of longer wavelength plasmon and the decrease in intensity of the 526 nm plasmon may be due to the adsorption of chlorpyrifos on the Au@citrate surface.[27] Figure 1B shows the photographs of Au@citrate (a), Au@citrate/Na_2SO_4 mixture (b) and the mixture with 12, 25, 125 and 250 ppb chlorpyrifos (c-f), respectively. The wine red color of the Au@citrate turns to purple by the addition of Na_2SO_4 solution. In the mixture with 12 ppb chlorpyrifos, the color remains purple. But in 25 ppb chlorpyrifos solution, the color immediately changes to blue. For 125 and 250 ppb chlorpyrifos, the color change is very fast. Thus visual observation of the presence of pesticide is possible. Figure 1C shows the plot of wavelength of absorption maximum versus chlorpyrifos concentration and the linear dynamic range of calibration is 20–125 ppb. The high correlation coefficient of 0.993 shows the linear relationship between chlorpyrifos concentration and maximum wavelength. The excellent reproducibility of the measurements was confirmed by the lower values of relative standard deviations (<1%). The lower detection limit (LOD) was found to be 10.8 ppb, which was calculated using the equation, LOD = 3S/m, where 'm' is the slope of the calibration curve and 'S' is the standard deviation for reference signal.[13]

UV-vis spectra of Au@citrate before and after the addition of malathion are shown in Figure 2A. Trace 'a' is the UV-vis spectrum of Au@citrate. Trace 'b' is the UV-vis spectrum of Au@citrate with Na_2SO_4. Trace 'c' is the UV-vis spectrum of 25 ppb malathion in Au@citrate/Na_2SO_4 mixture. Traces 'd-f' are the UV-vis spectra of 125, 250 and 500 ppb malathion solution in Au@citrate/Na_2SO_4 mixture, respectively. Traces 'b' and 'c' are almost the same and they showed characteristic absorption at 526 nm. But from 125 ppb onwards, the intensity of the 526 nm plasmon absorption started decreasing and an additional peak emerged at longer wavelength. The additional peak showed bathochromic shift and an increase in intensity with respect to the increase in concentration. The photograph of Au@citrate (a), Au@citrate/Na_2SO_4 mixture (b) and malathion-Au@citrate/Na_2SO_4 mixture (c-f) are shown in Figure 2B. The wine red color of the Au@citrate turns to purple by the addition of Na_2SO_4. With 25 ppb malathion in the Au@citrate/Na_2SO_4 mixture, the color remains as purple. The presence of 125 ppb malathion solution changes it to blue. For 250 and 500 ppb malathion, the color change to blue is rapid. Figure 2C is the plot of wavelength of absorption maximum versus malathion concentration and the linear dynamic range of the calibration is 100 -250 ppb. The observed correlation coefficient is 0.99 and the relative standard deviation is less than 1%. The LOD calculated from calibration curve is 40.36 ppb.

In the absence of Na_2SO_4 there is no color change for Au@citrate by the addition of pesticide. Figure 3 shows the

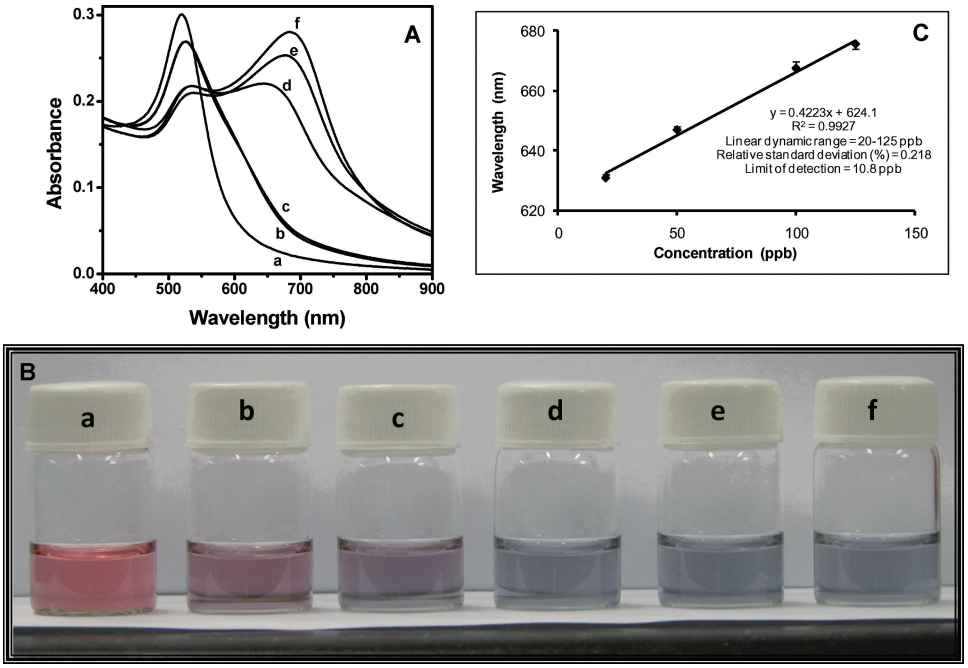

Fig. 1. (A) Ultraviolet-visible (UV-vis) spectra of Au@citrate before and after the addition of Na_2SO_4 and chlorpyrifos. Trace 'a' is the UV-vis spectrum of Au@citrate. Trace 'b' is the UV-vis spectrum of Au@citrate/Na_2SO_4 mixture. Traces 'c-f' are the UV-vis spectra of 12, 25, 125 and 250 ppb chlorpyrifos in Au@citrate/Na_2SO_4 mixture, respectively. (B) Photographs of Au@citrate before and after the addition of Na_2SO_4 and chlorpyrifos. (a) Au@citrate, (b) Au@citrate/Na_2SO_4mixture and (c-f) 12, 25, 125 and 250 ppb chlorpyrifos in Au@citrate/Na_2SO_4 mixture, respectively. (C) Plot of the wavelength of second plasmon absorption versus chlorpyrifos concentration.

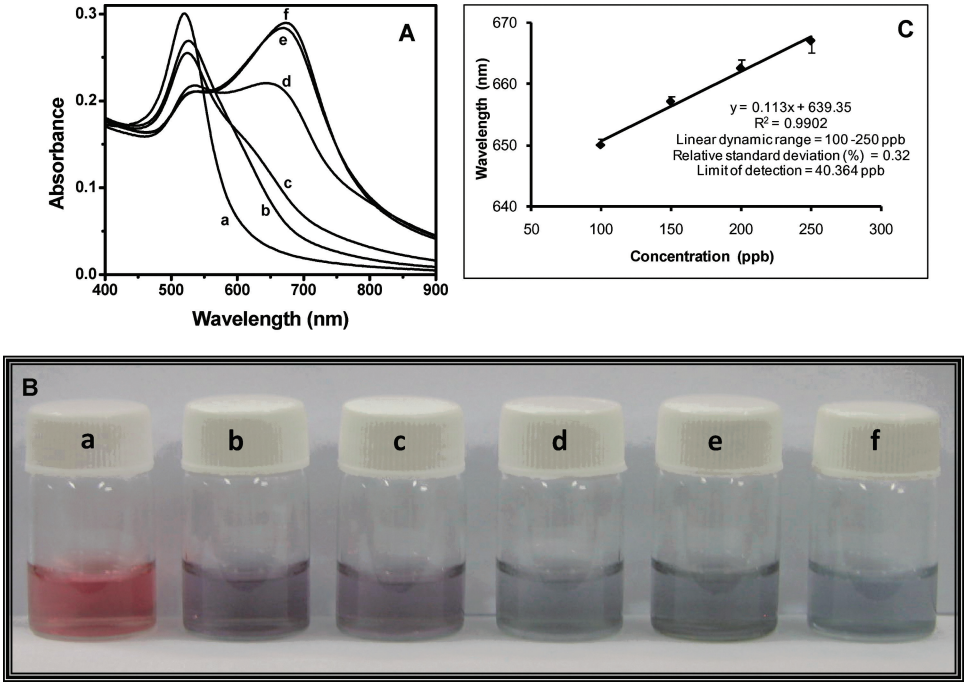

Fig. 2. (A) Ultraviolet-visible (UV-vis) spectra of Au@citrate before and after the addition of Na_2SO_4 and malathion. Trace 'a' is the UV-vis spectrum of Au@citrate. Trace 'b' is the UV-vis spectrum of Au@citrate/Na_2SO_4 mixture. Traces 'c-f' are the UV-vis spectra of 25, 125, 250 and 500 ppb malathion in Au@citrate/Na_2SO_4 mixture, respectively. (B) Photographs of Au@citrate before and after the addition of Na_2SO_4 and malathion. (a) Au@citrate, (b) Au@citrate/Na_2SO_4 mixture and (c to f) 25, 125, 250 and 500 ppb malathion in Au@citrate/Na_2SO_4 mixture, respectively. (C) Plot of the wavelength of second plasmon absorption versus malathion concentration.

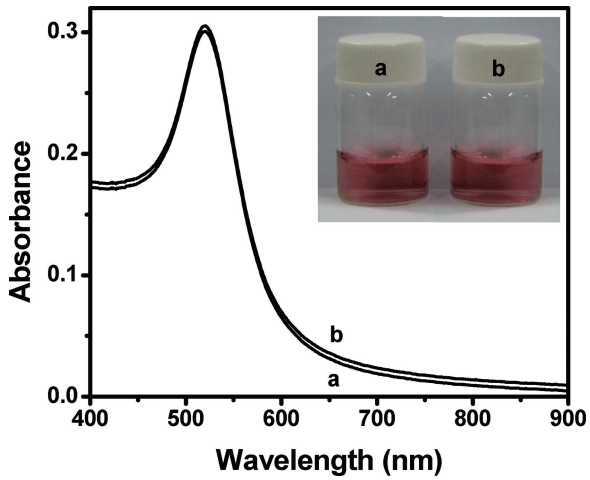

Fig. 3. Ultraviolet-visible (UV-vis) spectra of Au@citrate before and after the addition of chlorpyrifos. Trace 'a' is the UV-vis spectrum of Au@citrate and trace 'b' is the UV-vis spectrum of Au@citrate with 250 ppb chlorpyrifos. Inset is the photograph of Au@citrate before and after the addition of chlorpyrifos, (a) Au@citrate and (b) Au@citrate with 250 ppb chlorpyrifos.

UV-vis spectra of Au@citrate before and after the addition of chlorpyrifos solution. Trace 'a' is the UV-vis spectrum of Au@citrate and trace 'b' is 250 ppb chlorpyrifos in Au@citrate. Both the spectra are exactly the same and show the characteristic absorption at 520 nm, attributed to LSPR of Au@citrate. The concentration of chlorpyrifos is not enough to change the surface properties of Au@citrate particles. Inset is the photograph of Au@citrate before and after the addition of chlorpyrifos. The colors are same for both before and after adding chlorpyrifos.

The response of other salts to color change is not as good as compared to Na_2SO_4. By adding salts like NaCl, K_2SO_4 and $(NH_4)_2SO_4$, the time required for the color change is longer. Similarly, the detection limit is also high-i.e. 125 ppb for chlorpyrifos and 250 ppb for malathion.

Analysis of ground water

Table 1 shows the quality parameters of ground water used for the analysis. The UV-vis spectra of Au@citrate/Na_2SO_4 mixture before and after the addition of chlorpyrifos-

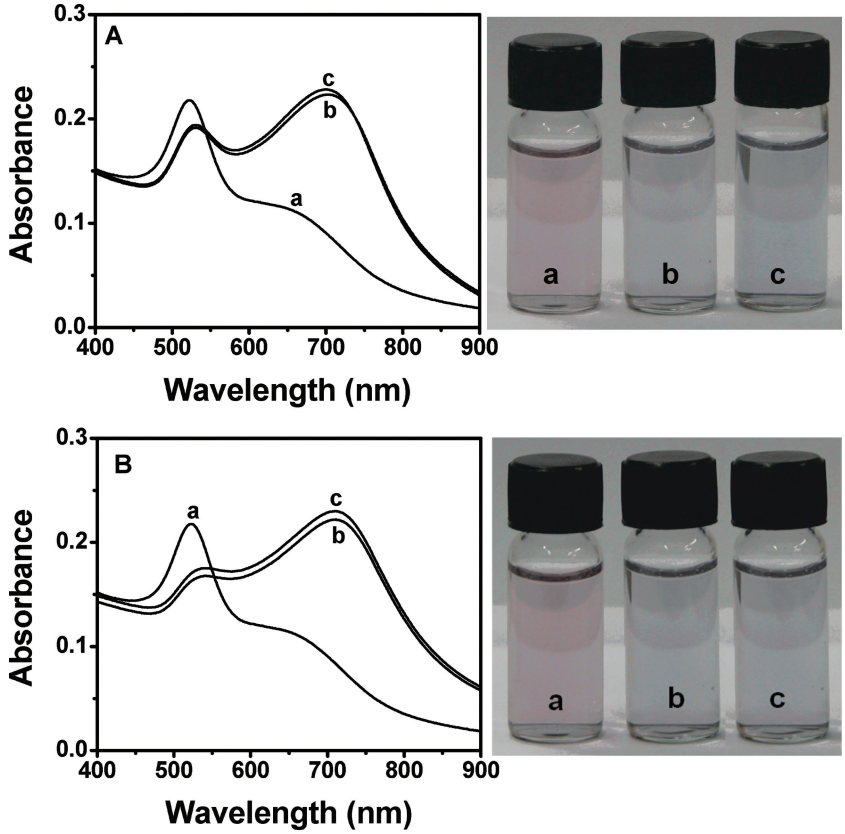

Fig. 4. (A) Ultraviolet-visible (UV-vis) spectra of Au@citrate/Na_2SO_4 mixture before and after the addition of chlorpyrifos-spiked water. Trace 'a' is the UV-vis spectrum of Au@citrate/Na_2SO_4 mixture. Traces 'b' and 'c' are the UV-vis spectra of 20 and 25 ppb chlorpyrifos in Au@citrate/Na_2SO_4 mixture, respectively. Photographs are of (a) Au@citrate/Na_2SO_4 mixture and (b, c) 20 and 25 ppb chlorpyrifos in Au@citrate/Na_2SO_4 mixture, respectively. (B) UV-vis spectra of Au@citrate/Na_2SO_4 mixture before and after the addition of malathion-spiked water. Trace 'a' is the UV-vis spectrum of Au@citrate/Na_2SO_4 mixture. Traces 'b' and 'c' are the UV-vis spectra of 120 and 125 ppb malathion in Au@citrate/Na_2SO_4 mixture, respectively. Photographs are of (a) Au@citrate/Na_2SO_4 mixture and (b, c) 120 and 125 ppb malathion in Au@citrate/Na_2SO_4 mixture, respectively.

Table 1. Quality parameters of the ground water sample used for the study.

Parameters	*Quantity*
pH @ 25 °C	8.01
Fluoride	2.30 ppm
Total alkalinity (as $CaCO_3$)	217 ppm
Total hardness (as $CaCO_3$)	178 ppm
Conductivity @ 25 °C	565 μmhos/cm
Organic carbon	< 0.5 ppm
Total Dissolved Solids	384 ppm
Calcium (as Ca)	36 ppm
Magnesium (as Mg)	22 ppm
Sulfate (as SO_4)	25 ppm
Chloride (as Cl^{-1})	13 ppm
Phosphate (as PO_4^{-3})	<0.02 ppm
Iron (as Fe)	<0.001 ppm
Nitrate (as NO_3^-)	38.9 ppm
Turbidity (as NTU)	0.2 NTU
Silica (as SiO_2)	47.4 ppm
Manganese	<0.001 ppm

spiked water are shown in Figure 4A. Trace 'a' is the UV-vis spectrum of Au@citrate/Na_2SO_4 mixture. The presence of absorbance at 565 nm, in addition to the characteristic absorption of gold nanoparticles, may be due to the presence of other ions in water. Traces 'b' and 'c' are the UV-vis spectra of 20 and 25 ppb chlorpyrifos in Au@citrate/Na_2SO_4 mixture. The appearance of a broad plasmon absorption at higher wavelength indicates the presence of chlorpyrifos. The photographs are corresponding to Au@citrate/Na_2SO_4 mixture (a) and chlorpyrifos-Au@citrate/Na_2SO_4 mixture (b, c). The color change of samples spiked with chlorpyrifos is obvious. Figure 4B shows the UV-vis spectra of Au@citrate/Na_2SO_4 mixture before and after the addition of malathion-spiked water. Trace 'a' is the UV-vis spectrum of Au@citrate/Na_2SO_4 mixture. Traces 'b' and c' are the UV-vis spectra of 100 and 125 ppb malathion in Au@citrate/Na_2SO_4 mixture and the plasmon of longer wavelength is observable. The photograph of Au@citrate/Na_2SO_4 mixture (a) and malathion-Au@citrate/Na_2SO_4 mixture (b, c) are shown in the figure.

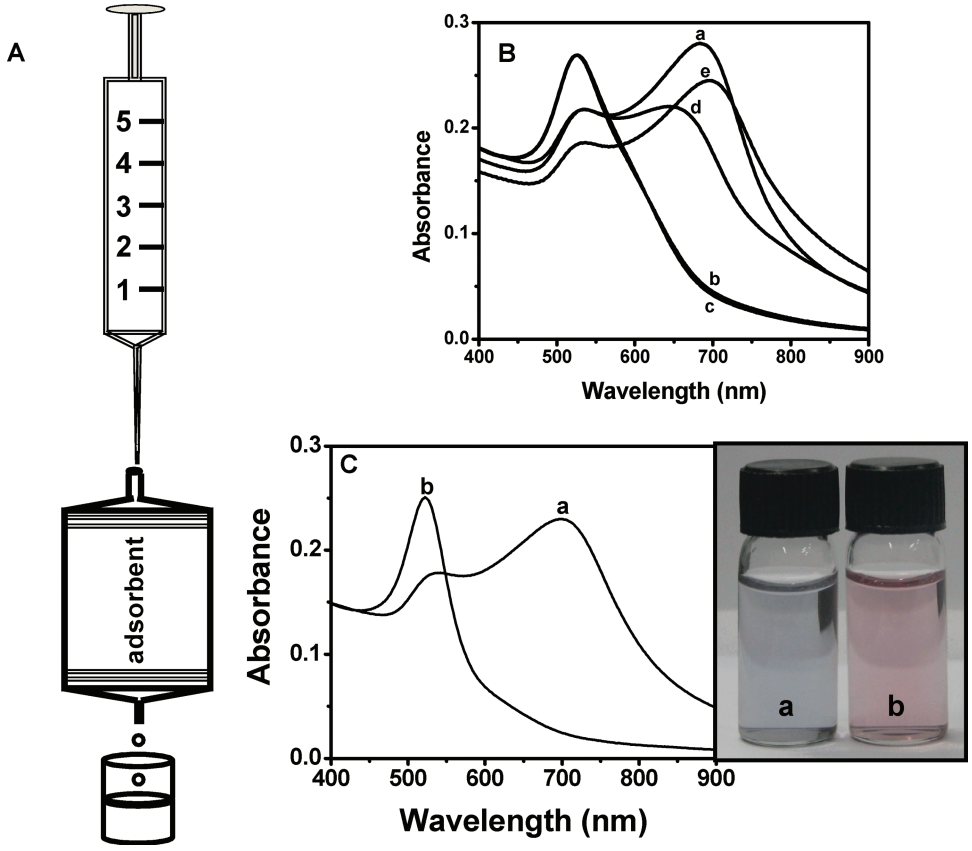

Fig. 5. (A) Schematic representation of the syringe filter used for chlorpyrifos removal. (B) Ultraviolet-visible (UV-vis) spectra of chlorpyrifos solution before and after passing through the filter. Trace 'a' is the UV-vis spectrum of 1 ppm chlorpyrifos (input) mixed with Au@citrate/Na_2SO_4 mixture. Traces 'b-e' are the UV-vis spectra of the eluent mixed with Au@citrate/Na_2SO_4 mixture corresponding to the passage of 50, 100, 110 and 125 mL, respectively. (C) UV-vis spectra of ground water spiked with chlorpyrifos and malathion before and after passing through the filter. Trace 'a' is the UV-vis spectrum of 1 ppm each chlorpyrifos and malathion (input) mixed with Au@citrate/Na_2SO_4 mixture. Trace 'b' is the UV-vis spectra of the eluent mixed with Au@citrate/Na_2SO_4 mixture. Photographs are of (a) 1 ppm each chlorpyrifos and malathion with Au@citrate/Na_2SO_4 mixture and (b) eluent with Au@citrate/Na_2SO_4 mixture, respectively.

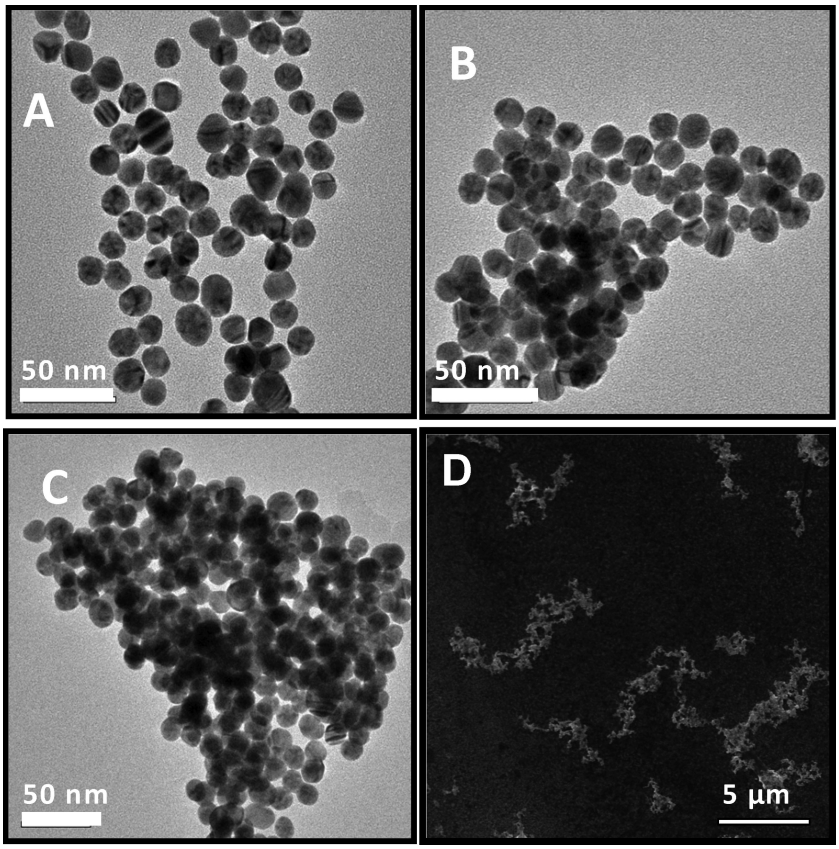

Fig. 6. High Resolution Transmission Electron Microscopy (HRTEM) images of (A) Au@citrate, (B) Au@citrate after the addition of Na_2SO_4 (C) Au@citrate/Na_2SO_4 mixture with 250 ppb chlorpyrifos and (D) SEM image Au@citrate/Na_2SO_4 mixture with 250 ppb chlorpyrifos.

The change in color in presence of malathion is clearly distinguishable.

Detection of treated samples

Silver nanoparticle-coated alumina showed a very high chlorpyrifos adsorption capacity.[27] Figure 5A shows a schematic diagram of a syringe filter unit used for extraction and detection studies of chlorpyrifos. The filter unit used was 3.5 cm in length and 1.5 cm in diameter. The adsorbent, silver nanoparticle-coated alumina, was packed in it. The flow of pesticide solution through the filter unit was controlled by the syringe. Figure 5B shows the UV-vis spectra of the solution after interaction with Au@citrate/Na_2SO_4 mixture. For this, output water was collected after passing definite volume of 1 ppm chlorpyrifos through the syringe filter. Trace 'a' shows the absorption spectrum when 1 ppm chlorpyrifos was mixed with Au@citrate/Na_2SO_4 mixture. Traces 'b-e' are the absorption spectra of the eluent collected after passing 50, 100, 110 and 125 mL chlorpyrifos solution, respectively. The 50 and 100 mL sample after mixing with Au@citrate/Na_2SO_4 mixture appeared in purple color. The spectra of these samples showed the plasmon absorption at 526 nm alone which is a clear evidence of the absence of chlorpyrifos. But from 110 mL onwards blue color appeared in samples by mixing with Au@citrate/Na_2SO_4 mixture and the spectra showed the emergence of plasmon absorption at longer wavelength, which indicated that the presence of chlorpyrifos is detectable by this method. Figure 5C shows the UV-vis spectra of real water samples spiked with pesticides before and after passing through the silver nanoparticle-coated alumina filter. Trace 'a' is the absorption spectrum for a mixture of 1 ppm each chlorpyrifos and malathion in Au@citrate/Na_2SO_4 mixture. Trace 'b' is the absorption spectrum of the sample after passing through the filter (along with Au@citrate/Na_2SO_4 mixture). It matches exactly with the spectrum obtained for analysis with distilled water. The photographs of sample before (a) and after (b) passing through the filter (along with Au@citrate/Na_2SO_4 mixture) are shown in the figure. The color change of the sample before and after the treatment is apparent.

HRTEM and SEM analyses

HRTEM images show the effect of addition of Na_2SO_4-pesticide solution into Au@citrate. Figure 6A is the HRTEM image of Au@citrate. The nanoparticles are

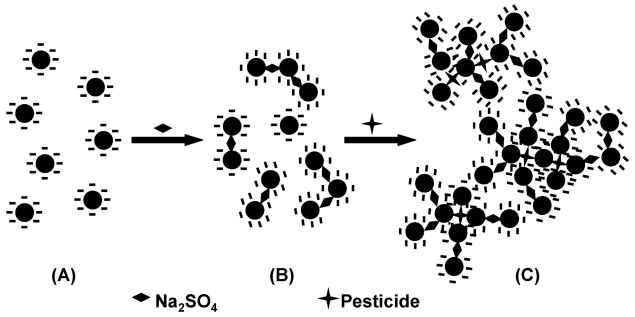

Fig. 7. Schematic representation of the changes in the Au@citrate by the addition of Na_2SO_4 and pesticide. (A) Au@citrate, (B) Au@citrate after the addition of Na_2SO_4 and (C) Au@citrate after the addition of Na_2SO_4 and pesticide.

spherical in shape and are uniformly distributed as typical of citrate synthesis. Their size distribution is remarkably narrow and all particles are within 16 ± 2 nm. Figure 6B is the HRTEM image of Au@citrate treated with Na_2SO_4 which shows the aggregation of nanoparticles. Figure 6C is the HRTEM image of Au@citrate/ Na_2SO_4 mixture with 250 ppb chlorpyrifos. The particles are highly aggregated by the addition of chlorpyrifos. SEM image of the Au@citrate/Na_2SO_4 mixture with 250 ppb chlorpyrifos is shown in Figure 6D. The highly aggregated morphology is clear in the image.

A schematic representation of the sequence of changes by the addition of Na_2SO_4 and the pesticide molecules into Au@citrate is shown in Figure 7. The aggregation and respective color changes are indicated. Scheme (A) represents Au@citrate. (B) and (C) represent Au@citrate with Na_2SO_4 and Na_2SO_4/pesticide mixture, respectively. Increased aggregation is suggested to be the reason for the distinct color change with pesticides.

Au@citrate assisted colorimetric method proposed here does not require any expensive chemicals and the response occurs within 2 minutes. For a typical test, only a few mL Au@citrate is needed and the cost of the entire test is under 2 Indian Rupees or 2.5 cents. The rapid screening possibility, long term stability of the reagents at atmospheric conditions and their non-toxic nature are added advantages of this method for the on-site visual detection of chlorpyrifos and malathion. Pesticide detection kit can be developed on the basis of this and is useful for demonstrating the performance of pesticide removing materials and filters.

Conclusions

Gold nanoparticle treated with Na_2SO_4 is an effective system for the visual detection of chlorpyrifos and malathion up to ppb levels. The response of this method is observable as a color change and is very fast. UV-vis spectroscopy, HRTEM and SEM analysis were used for understanding the mechanism. Tests with ground water samples show the usefulness of the system in real-life situations. Although it is necessary to lower the limits further, the current study shows that reasonable monitoring is achievable even with the visual detection method.

Acknowledgment

We thank Department of Science and Technology, Government of India for constantly supporting our research program on nanomaterials.

References

[1] Costa, L.G. Current issues in organophosphate toxicology. Clin. Chim. Acta. **2006**, *366*, 1–13.
[2] World Health Organization (WHO). WHO/SDE/WSH/03.04/103; 2004. http://www.who.int/water_sanitation_health/dwq/chemicals/malathion.pdf (accessed Aug 2008).
[3] Zeljezic, D.; Vrhovac, V.G. Sister chromatid exchange and proliferative rate index in the longitudinal risk assessment of occupational exposure to pesticides. Chemosphere. **2002**, *46*, 295–303.
[4] Rosen, R. Mass spectrometry for monitoring micropollutants in water. Curr. Opin. Biotech. **2007**, *18*, 246–251.
[5] Sancho, J.V.; Pozo, O.J.; Ibanez, M.; Hernandez, F. Potential of liquid chromatography/time-of-flight mass spectrometry for the determination of pesticides and transformation products in water. Anal. Bioanal. Chem. **2006**, *386*, 987–997.
[6] van der Hoff, G.R.; van Zoonen, P. Trace analysis of pesticides by gas chromatography. J. Chromatogr. A. **1999**, *843*, 301–322.
[7] Balinova, A. Strategies for chromatographic analysis of pesticide residues in water. J. Chromatogr. A. **1996**, *754*, 125–135.
[8] Jiang, X.; Li, D.; Xu, X.; Ying, Y.; Li, Y.; Ye, Z.; Wang, J. Immunosensors for detection of pesticide residues. Biosens. Bioelectron. **2008**, *23*, 1577–1587.
[9] Rogers, K.R. Recent advances in biosensor techniques for environmental monitoring. Anal. Chim. Acta. **2006**, *568*, 222–231.
[10] Andreescu, S.; Marty, J.L. Twenty years research in cholinesterase biosensors: From basic research to practical applications. Biomol. Eng. **2006**, *23*, 1–15.
[11] Mulvaney, P. Surface plasmon spectroscopy of nanosized metal particles. Langmuir. **1996**, *12,* 788–800.
[12] Hutter, E.; Fendler, J.H. Exploitation of localized surface plasmon resonance Adv. Mater. **2004**, *16*, 1685–1706.
[13] Rex, M.; Hernandez, F.E.; Campiglia, A.D. Pushing the limits of mercury sensors with gold nanorods. Anal. Chem. **2006**, *78*, 445–451.
[14] Chen, J.; Zheng, A.F.; Chen, A.H.; Gao, Y.; He, C.; Kai, X.; Wu, G.; Chen, Y. A functionalized gold nanoparticles and Rhodamine 6G based fluorescent sensor for high sensitive and selective detection of mercury(II) in environmental water samples. Anal. Chim. Acta. **2007**, *599*, 134–142.
[15] Huang, C.C.; Chang, H.T. Selective gold-nanoparticle-based "Turn-On" fluorescent sensors for detection of mercury(II) in aqueous solution. Anal. Chem. **2006,** *78*, 8332–8338.
[16] Kim, Y.; Johnson, R.C.; Hupp, J.T. Gold nanoparticle-based sensing of "spectroscopically silent" heavy metal ions. Nano Lett., **2001**, *1*, 165–167.
[17] Zhou, Y.; Wang, S.; Zhang, K.; Jiang, X. Visual detection of copper(II) by azide- and alkyne-functionalized gold nanoparticles using click chemistry. Angew. Chem. Int. Ed. **2008**, *47*, 7454–7456.
[18] Nair, A.S.; Tom, R.T.; Pradeep, T. Detection and extraction of endosulfan by metal nanoparticles. J. Environ. Monit. **2003**, *5*, 363–365.

[19] Lin, T.J.; Huang, K.T.; Liu, C.Y. Determination of organophosphorous pesticides by a novel biosensor based on localized surface plasmon resonance. Biosens. Bioelectron. **2006**, *22*, 513–518.

[20] Shulga, O.; Kirchho, J.R. An acetylcholinesterase enzyme electrode stabilized by an electrodeposited gold nanoparticle layer. Electrochem. Commun. **2007**, *9*, 935–940.

[21] Du, D.; Chen, S.; Cai, J.; Zhang, A. Electrochemical pesticide sensitivity test using acetylcholinesterase biosensor based on colloidal gold nanoparticle modified sol-gel interface. Talanta, **2008**, *74*, 766–772.

[22] Du, D.; Ding, J.; Cai, J.; Zhang, A. One-step electrochemically deposited interface of chitosan-gold nanoparticles for acetylcholinesterase biosensor design. J. Electroanal. Chem. **2007**, *605*, 53–60.

[23] Dasary, S.S.R.; Rai, U.S.; Yu, H.; Anjaneyulu, Y.; Dubey, M.; Ray, P.C. Gold nanoparticle based surface enhanced fluorescence for detection of organophosphorus agents. Chem. Phys. Lett. **2008**, *460*, 187–190.

[24] Enustun, B.V.; Turkevich, J. Coagulation of colloidal gold. J. Am. Chem. Soc. **1963**, *85*, 3317–3328.

[25] Kamat, P.V.; Flumiani, M.; Hartland, G.V. Picosecond dynamics of silver nanoclusters. Photoejection of electrons and fragmentation. J. Phys. Chem. B. **1998**, *102*, 3123–3128.

[26] Burns, C.; Spendel, W.U.; Puckett, S.; Pacey, G.E. Solution ionic strength effect on gold nanoparticle solution color transition. Talanta. **2006**, *69*, 873–876.

[27] Nair, A.S.; Pradeep, T. Extraction of chlorpyrifos and malathion from water by metal nanoparticles. J. Nanosci. Nanotechno. **2007**, *7*, 1–7.